Interpretation of Molecular Structure and Kinetics in Melt Condensation of A_2 Oligomers, B_3 Monomers, and Monofunctional Reagents

C. Oguz,[†] S. Unal,[§] T. E. Long,[‡] and M. A. Gallivan*,[†]

School of Chemical & Biomolecular Engineering, Georgia Institute of Technology, Atlanta, Georgia 30332; Department of Chemistry, Virginia Tech, Blacksburg, Virginia 24061; and Bayer MaterialScience, Pittsburgh, Pennsylvania 15205

Received January 26, 2007; Revised Manuscript Received June 13, 2007

ABSTRACT: This article applies kinetic Monte Carlo simulations to interpret experimental measurements in the polymerization of hyperbranched poly(ether esters)s in a melt condensation of A_2 oligomers and B_3 monomers. Building on the analytical modeling of Flory and Stockmayer, additional effects of cycle formation, unequal reactivities, and end-capping reagents are added into the simulations to describe $A_2 + B_3$ polymerization in the absence of a solvent. The experimental data have been published separately,[1] and here it is compared to the model predictions in order to quantitatively assess whether the data are consistent with these models. On the basis of the modeling, we conclude that cycle formation is negligible, suppression of the third B group is insignificant, and the mobility of the free B_3 monomer leads to enhancement of its reaction rate. The addition of the monofunctional end-capping reagents does not necessarily lead to suppression of branching in the $A_2 + B_3$ system and depends sensitively on the stoichiometry of the reactants.

I. Introduction

The shape and topology of organic molecules have a profound effect on their properties.[2] In the past two decades, synthetic polymer chemists have introduced a new class of highly branched macromolecules which are composed of multifunctional monomers and are classified as either dendrimers or hyperbranched polymers. Dendrimers are typically synthesized using multistep reactions, and they offer superior control of molecular size, shape, and functionality. On the other hand, hyperbranched polymers are less ordered but are easier to synthesize.

Discussion of the synthetic methodologies for preparation of a wide range of hyperbranched and dendritic polymers can be found in several extensive review articles.[3−5] Many of the past experimental studies have focused on the synthesis and characterization of AB_n-type monomers ($n \geq 1$), particularly with AB_2 monomers.[3−6] However, very few of the AB_n-type monomers are commercially available due to their lack of symmetrical functionality and tendency to react prematurely.[4] As a result, $A_2 + B_3$ polymerization has recently been the subject of extensive research[7−14] since it provides an alternative and more convenient way to synthesize highly branched polymers. In contrast to polymerization of AB_n-type monomers, these systems offer a wider range of molecular structures depending on the monomeric types and processing conditions. For example, $A_2 + B_3$ polymerization has been performed by heating a mixture of $A_2 + B_3$[1] and also by dropwise addition of A_2 into B_3.[15] The molar ratio of A_2 to B_3 can also be varied.[4,16,17] Moreover, our recent efforts have demonstrated the opportunity to control the distance between branch points through the judicious selection of various telechelic oligomers as A_2.

Modeling studies have long been used to explain experimental observations in an adhoc fashion, and modeling is often used to steer the discovery of synthetic methods and the formation of novel architectures. Early work of Flory[16] and Stockmayer[18,19] on the step growth of multifunctional monomers was based on the assumption that there was no cycle formation in these polymerization processes, which enabled the calculation of molecular weight using an infinite series solution. The models of Flory and Stockmayer are useful because they enable quantitative predictions of polymer properties. While it is intuitive that a branched polymer that is composed of A_2 and B_3 monomers will ultimately gel, the model generates the quantitative prediction of gelation at 87% A conversion for the stoichiometry of A_2:B_3 = 1:1.[19] More recently, this method has been extended to include the effect of cycle-forming reactions on the gel point.[20]

In order to predict the time evolution of polymerization, kinetic models based on mass-action kinetics are often employed. Ordinary differential equations are used to describe the concentration of each type of branching unit.[21,22] For example, a trifunctional monomer may exist in four states: no reactions (free), one reaction (terminal), two reactions (linear), and fully reacted (dendritic). These models are typically of low dimension and may be solved analytically in some cases or numerically in others. A disadvantage of this modeling approach is that no information is provided on the molecular weight distribution of the resulting polymer.

When prediction of the molecular weight and its distribution is also desired, population balance models are commonly used, in which the concentration of polymers of each possible size is computed.[17,21,23−25] These models therefore have high dimension. For systems of linear polymers composed of a single monomer type, the kinetics are fully described by the number of monomers in the polymer. Thus, if one models the concentration of polymers up to a maximum size of 1000 monomeric units, then the dimension of the model is also 1000. However, in branched polymers, more information is needed to describe the kinetics, such as the number of reactive end groups in the polymer. When several descriptors are needed to describe each polymer, the dimension of the population balance model grows rapidly.[17] For the model considered in this article, six descriptors are used to describe each polymer: the number of A_2 monomers, the number of B_3 monomers, the number of unreacted A groups in the polymer, the number and type of unreacted B groups (linear or terminal), and the number of end-capping agents.

* Corresponding author.
[†] Georgia Institute of Technology.
[‡] Virginia Tech.
[§] Bayer MaterialScience.

10.1021/ma070225v CCC: $37.00
Published on Web 08/04/2007

Solving a population balance model with six descriptors would be very intensive computationally.

Generating functions and the method of moments are often used to reduce the dimension of these population balance models. However, this approach becomes much more difficult as the number of descriptors grows, since moments must be included for each descriptor. The difficulty of this approach is illustrated by the recent paper of Dusek, Duskova-Srmckova, and Voit,[17] in which unequal reactivities and monofunctional reagents were considered separately but not simultaneously.

Cycle formation was neglected by Flory and Stockmayer, but it is a major factor in the structural development of dendritic and hyperbranched polymers.[23,25−28] The method of moments has been extended to describe cycle formation in hyperbranched polymers composed of AB_2 monomers[25] and the $AB_2 + B_3$ system.[29] This extension is enabled because in these systems a maximum of one cycle is possible, at which point the polymer cannot grow further. In contrast, in the $A_2 + B_3$ system, there is no limit on the maximum number of cycles. Infinite series solutions have been developed to predict the gel point in the $A_2 + B_3$ system but do not include additional effects such as unequal reactivities of the groups in B_3 and the effect of monofunctional reagents.[20]

As an alternative to mass action kinetic models that use concentration variables, Monte Carlo simulations have been performed for hyperbranched polymers, so that more realistic kinetics can be included and so that structural information can be obtained. For example, the Wiener index can be computed for each polymer in the simulation, which is related to viscosity.[30] In the Monte Carlo simulations, individual monomers are reacted with each other to build up the polymer, using random numbers to select each event. Each monomer is tracked throughout the simulation, and information regarding its connection to other monomers is stored. Monte Carlo simulations may be used to describe only the connectivity of the polymers, without describing their spatial positions,[15,25,29,31] or lattice Monte Carlo simulations can be performed in which each monomer is associated with a spatial position in the lattice.[32] Direct comparison between experimental data and Monte Carlo simulations has been limited to date, but these simulations can be valuable in interpreting experimental results.[15,25] As computational resources grow, Monte Carlo simulations become an increasingly attractive alternative to population balance modeling, since their major drawback has been the amount of computation required.

Another modeling approach is to describe the structural development of hyperbranched polymers using atomistically detailed algorithms.[2,30] These studies are limited to the growth of single polymers at a time because of the high computational cost, so they are not as useful for predicting the molecular weight distribution. However, if the conformation of the polymer changes throughout the reaction and this strongly influences the kinetics, then it may be necessary to include this level of detail.

Recent studies employ syntheses of hyperbranched polymers via $A_2 + B_3$ both in a solution[7−9,12] and also in the melt phase[1,33] with no solvent. Herein, we combine experimental and computational efforts to understand the polymer structural development in a melt, especially branching and the onset of gelation. The experimental data have been published previously,[1] and this paper employs a Monte Carlo simulation to interpret the experimental findings and to eludicate the underlying kinetics. In a previous study, we used a simpler kinetic model to explore the role of cyclization in the dropwise addition of A_2 into B_3 in a solvent.[15] Herein we consider a similar statistical framework to explore a wider range of phenomena, for a batch $A_2 + B_3$ reaction in a melt. The Monte Carlo simulations are used to interpret the experimentally measured number-averaged molecular weight, weight-averaged molecular weight, and the density of branched units, by considering the effects of the cyclization reactions, unequal reactivities, and end-capping on the structure development of hyperbranched polymers.

II. Experimental Section

Highly branched poly(ether ester)s were synthesized in the melt phase using an oligomeric $A_2 + B_3$ polymerization strategy. Condensation of poly(propylene glycol) (A_2 oligomer) and trimethyl 1,3,5-benzenetricarboxylate (B_3 monomer) generated highly branched structures. The conversion and degree of branching were measured with ^{1}H NMR spectroscopy, and the molecular weight (number-average, weight-average, and polydispersity) was characterized using size exclusion chromatography (SEC), at six points throughout the polymerization process. Additional experiments were also performed in which two different monofunctional end-capping reagents were added for the purpose of delaying the gel point. This experimental work has been published previously[1] and should be consulted for further details on the experimental procedures. The present work interprets these experiments through a comparison with Monte Carlo simulations, utilizing alternative assumptions and kinetic models. Because the error in the SEC measurements is ~10%, our goal is not to achieve exact agreement between the experiments and modeling but to compare the trends and magnitudes.

III. Model and Simulations

This paper focuses on the use of a model to interpret the experimental data. Each simulation starts with N monomers of A_2 and N monomers of B_3 in the system, since the monomers were polymerized with a 1:1 molar ratio during the experiments. At each step in the simulation, all of the available (unreacted) functional groups are listed. Then, using a random number, an A group and a B group are selected from the list and the reaction is executed. This is followed by updating the list of available A and B groups, molecular weights of the molecules, and the number of dendritic, linear, and terminal units in the system.

The probability of selecting a particular pair of A and B groups is proportional to the reaction rate for that pair, which yields the correct time evolution of the system.[34] Therefore, a model is needed for the reaction rates of various events. The first effect that is considered in this effort is the formation of cycles through intramolecular reactions. Our polymerization was performed in the melt, which was hypothesized to minimize cycle formation due to high concentration of reactants, so cyclization reactions are taken into account in the simulations to address this hypothesis. While selecting an A group (from A_2 oligomers) and a B group (from B_3 monomers) for reaction at each simulation step, some pairs are favored more than the others. If the reaction of an A−B pair leads to cycle formation, the selection probability of that particular pair is promoted by the cyclization parameter γ, such that $\gamma = (k_c/k_{nc})/N$, where k_c is the rate of cyclization reactions for each A−B pair and k_{nc} is the rate of noncyclization reactions for each A−B pair. N appears in the parameter γ since the number of intermolecular reactions in the simulations grows as N^2, while intramolecular reactions are initially proportional to N. Although γ is constant throughout each simulation, the overall number of cycle-forming reactions increases with conversion because the number of possible cycle-forming reactions increases with molecular weight. We use different values of γ in the simulations to explore the effect of cycle formation on the resulting polymer.

In addition to cyclization and noncyclization reactions, we also consider end-capping reactions between E groups (from

monofunctional end-capping reagents) and B groups, with a rate constant of k_e. The ratio $\epsilon = k_e/k_{nc}$ is then the second parameter in our kinetic model. In a second set of simulations, γ and ϵ have been varied to observe their effects on the development of molecular characteristics such as number-average molecular weight (M_n), weight-average molecular weight (M_w), polydispersity index (PDI $= M_w/M_n$), and the fraction of dendritic units (f_D). f_D is calculated using $f_D = D/(D + T + L)$, where D, L, and T indicate the number of dendritic, linear, and terminal units in the system. We plot f_D in the simulation results (as opposed to f_L or f_T), since f_D is the quantity extracted from the ^{1}H NMR measurements.[1]

Depending on the properties of the monomers, such as their molar mass or electrostatic interactions, unequal reactivities of their groups can also affect the structural development of hyperbranched polymers. End groups usually have higher reactivities than the groups along the length of the chains because of the lower kinetic excluded volume effect.[35] This would cause the linear units to have lower reactivities than the terminal units. In order to simulate unequal reactivities of the B groups, we define a third parameter ρ. For each unreacted B group in a B_3 monomer, we check the reaction state of the other two B groups in the monomer. We then consider three possible cases of unequal reactivity. For this purpose, we define k_1 to be the rate of reaction of a B group in a free B_3 monomer, k_2 to be the rate of a B group in a terminal unit, and k_3 for a B group in a linear unit. We assign reaction rates in the ratio of $\rho = k_1/k_2 = k_2/k_3$. k_1 is expected to be enhanced relative to k_2 due to the greater mobility of the free B_3 monomer and its ability to diffuse through the polymer, while k_2 may be different from k_3 due to blocking, free volume, and electrostatic considerations. In order to isolate these two effects, we have also performed simulations with $\rho_{12} = k_1/k_2$ and $k_2 = k_3$ and then also with $\rho_{23} = k_2/k_3$ and $k_1 = k_2$.

For the simulation results presented in this study, the system size is $N = 10\,000$. Smaller simulation sizes of $N = 1000$, 3000, 5000, and 7000 have also been used. The simulation results with $N = 1000$ differ significantly from the simulations with larger N. On the other hand, simulations with larger N agreed quantitatively. This suggests that the trends reported in this study are not dependent on the system size. Additionally, for the case of no cycle formation and equal B_3 reactivity, we compared our weight-averaged molecular weight with the analytical theory of Stockmayer,[19] and the error is ~1%. Clearly, if one is interested in describing the approach to gelation with no bound on the molecular weight, then the system size would also need to approach a macroscopic number of monomers (10^{23}), and studies have been performed to quantify this tradeoff.[36] However, in these simulations, only molecular weights up to 500 000 g/mol are presented, since this is the range of the experimental data. Furthermore, the error in the SEC measurements is ~10%, so an error of 1% in the model predictions is not significant.

IV. Results and Discussion

Monte Carlo simulations have been carried out in order to assess the effects of cyclization, unequal reactivities, and end-capping reactions on the polymer structure development. Molecular weights of A_2 (PPG-1000) and B_3 (TMT) are 1060 and 252 g/mol, whereas the molecular weights of two types of end-capping reagents, PPG-M-1000 and dodecanol, are 1200 and 187 g/mol, respectively. The simulation system containing $10\,000 \times 10\,000$ A_2 and B_3 monomers yielded molecular weights in the same range as those observed in the experiments. Similar to the experiments, simulations have been initialized with an equal number of A_2 and B_3 monomers in the system. The simulation results plotted are averages over 50 independent realizations.

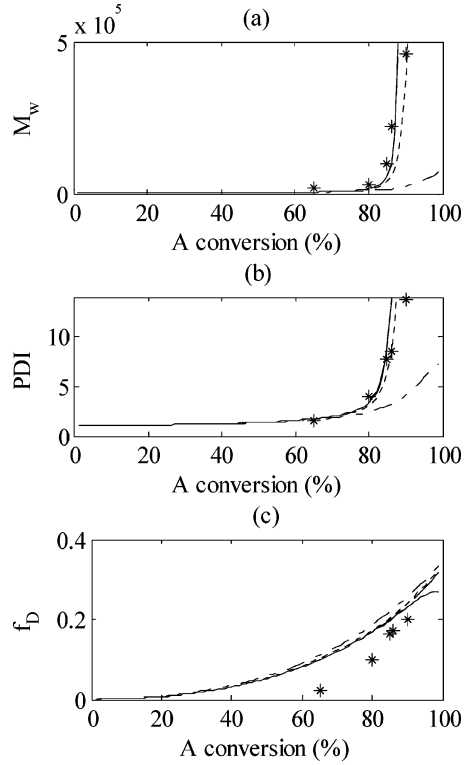

Figure 1. Comparison of simulation and experiment[1] (*). In the simulations, the cyclization ratio γ is varied: $\gamma = 0$ (solid line), $\gamma = 10^{-3}$ (dashed line), $\gamma = 10^{-2}$ (dotted line), $\gamma = 10^{-1}$ (dashed-dot line). (a) Weight-average molecular weight M_w, (b) polydispersity index PDI, and (c) fraction of dendritic units f_D. Agreement between experiments and simulations is not achieved for f_D at any value of γ.

a. Effects of Cyclization Reactions. The melt polymerization was previously considered to be sufficiently concentrated so that the cycle formation would be negligible.[1] We first investigate the extent of cyclization via the simulations. Extent of cyclization (EOC) is defined as the fraction of reactions between A and B that is intramolecular and is a quantity that has been measured previously using MALDI-ToF for linear polymers but is less reliably measured in hyperbranched polymers due to the many possible isomers.[14,37]

Figure 1a,b shows the experimental[1] and simulated evolution of the weight-average molecular weight M_w and the polydispersity PDI as a function of A_2 conversion, for the $10\,000 \times 10\,000$ $A_2 + B_3$ system with different γ values. The reactivity ratio ρ is 1, and no monofunctional reagents are present. For all γ values, a slow increase in M_w and PDI values was observed until about 80% A_2 conversion. Above 80% A_2 conversion, a sharp increase in M_w and PDI takes place in all the systems, except for the one with the highest level of cyclization ($\gamma = 1$). The experimental data for PDI and M_w are most consistent with a value of γ around 10^{-2}. The ideal limit of no cycle formation, modeled by Flory, is the solid curve with $\gamma = 0$.

M_w and PDI development in systems with cyclization ratios in the range of $\gamma = 0-10^{-2}$ all agree reasonably well with the experimental data. Because of the variability of the experimental measurements, the goal of the modeling is not to match the experiments exactly but to assess the magnitude of the various effects. The simulation with $\gamma = 10^{-1}$ has a lower M_w and PDI at high conversions compared to the experimental data. This suggested that the extent of cyclization, which is the fraction

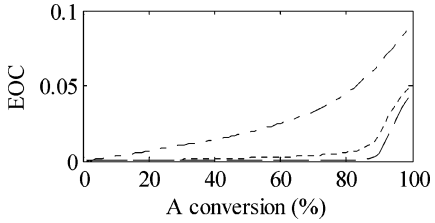

Figure 2. Simulation predictions of extent of cyclization. The cyclization ratio γ is varied: $\gamma = 10^{-3}$ (dashed line), $\gamma = 10^{-2}$ (dotted line), $\gamma = 10^{-1}$ (dashed-dot line). For the $\gamma = 0$ case, EOC = 0.

of reactions that are cycle-forming, was quite low during the experiment. Figure 2 shows that the system with $\gamma = 10^{-1}$ reaches an extent of cyclization of 0.09 at 90% A_2 conversion. Interestingly, even such a low extent of cyclization dramatically suppressed the M_w and PDI, as illustrated in Figure 1a,b. Figure 2 also shows that with $\gamma = 10^{-3}$ or $\gamma = 10^{-2}$ the extent of cyclization is less than 3%. This result supports the original hypothesis that melt polymerization would suppress the effect of cycle formation on molecular weight and gelation.

Another important characteristic of hyperbranched polymers is the fraction of dendritic units f_D, which is directly proportional to the extent of branching in the system. The development of f_D at different γ levels is shown in Figure 1c as a function of A_2 conversion. As γ is increased from $\gamma = 10^{-2}$ to $\gamma = 10^{-1}$, an increase in f_D is observed at A_2 conversions of 60% and above. This trend was expected since cyclization reactions enhance the number of dendritic groups via the formation of small, fully reacted polymers with no free groups. However, the evolution of f_D is not consistent with the experimental data for any value of γ. For all γ, the simulations predict a higher fraction of dendritic units.

b. Effects of Unequal Reactivities. The disagreement of f_D between the experiments and simulations suggests that there is an additional effect that suppresses the amount of branching during the experiments, other than the effect of cyclization reactions. It could be attributed to the lower reactivity of free B groups in linear units relative to the free B groups in the terminal units or completely unreacted B_3 monomers. However, this would also reduce the molecular weight. In order to assess this tradeoff quantitatively, additional simulations have been performed during which the reactivity of free B groups is modified, based on the overall state of the B_3 monomer. In these simulations presented in this section, $\gamma = 0$ since the previous section demonstrated that cyclization did not play a major role in this system.

Figure 3 shows the evolution of the simulations with different levels of reactivity ratio ρ. With $\rho = 1$, the simulations are identical to those in Figure 1, while larger ρ reduces the amount of branching and also the molecular weight and distribution. The reduction in molecular weight was expected since the polymers are becoming more linear, but the reduction of molecular weight and polydispersity is not as dramatic as it is with cyclization. Even for the extreme value of $\rho = 10$, gelation is delayed but not completely suppressed. In Figure 3c, the increase in ρ causes a decrease in f_D, as expected, but the shape of the curves does not match the experimental data. In the data, the fraction of dendritic units rises quite high at late conversion but is very low at earlier conversions. The 1:1 molar ratio of A_2 and B_3 is important in understanding this behavior. Because of the 1:1 molar ratio, there is an excess of B groups, so at full A conversion, only $^2/_3$ of the B groups have reacted. If the reactivity of the third B group is strongly reduced, then there will be few dendritic units that form, but this is not observed in

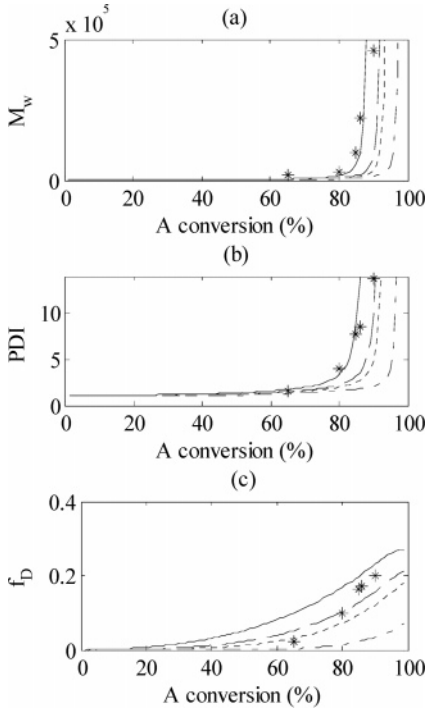

Figure 3. Comparison of simulation and experiment[1] (*). In the simulations, $\rho = k_1/k_2 = k_2/k_3$. $\rho = 1$ (solid line), $\rho = 1.5$ (dashed line), $\rho = 2$ (dotted line), $\rho = 10$ (dashed-dot line). (a) Weight-averaged molecular weight, (b) polydispersity index, and (c) fraction of dendritic units.

the experiments. The fact that the experiments eventually reach a large value of f_D near that predicted with $\rho = 1$ instead suggests that a B group in a linear unit has a similar reactivity to a B group in a terminal unit.

The low values of f_D around 60% conversion are more consistent with a suppression of the reaction of terminal units relative to free units, as shown in Figure 4 for various levels of ρ_{12}. Recall that $\rho_{12} = k_1/k_2$, with $k_2 = k_3$. The high reactivity of the free B_3 could be due to its mobility as well as the fact that B groups in polymers may be partially blocked by other portions of the polymer. This trend in f_D is much more consistent with the experimental data. A high value of $\rho_{12} = 10$ best matches the f_D measurements, while a somewhat lower value of ρ_{12} near 1.5−2 agrees best in the molecular weight distribution. Our conclusion based on the simulations in Figures 3 and 4 is that a suppressed reactivity of the third B group in the linear unit is not consistent with the observed data. The more consistent explanation is that the free B_3 monomers are more mobile and therefore react faster than B_3 in polymer.

c. Effects of End-Capping Reagents. The third and final simulation study considers the addition of monofunctional reagents to the $A_2 + B_3$ system. Stockmayer's theoretical studies of highly branched polymers indicated that addition of a monofunctional end-capping reagent should shift the gel point to higher monomer conversion values.[16,18,19] Thus, delaying the gel point by terminating some of the B functionalities is the main motivation behind using end-capping reagents in this system. A molar ratio of monomers as A_2:B_3:E = 1:1:1 was used in the experiments to ensure that residual B end groups, which would be expected in an A_2:B_3 = 1:1 system at full A_2 conversion, do not remain in the system at full conversion.

Figure 5 provides a comparison of the change in the evolution of M_w for the addition of PPG-M-1000 (1200 g/mol) at the beginning of the reaction. The A conversion that is plotted also includes the conversion of the end-capping reagent, since that

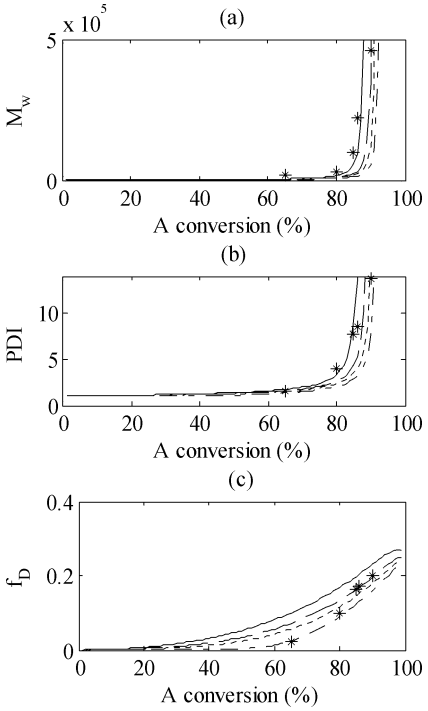

Figure 4. Comparison of simulation and experiment[1] (*). In the simulations, $\rho_{12} = k_1/k_2$ and $k_2 = k_3$. $r_{12} = 1$ (solid line), $\rho_{12} = 1.5$ (dashed line), $\rho_{12} = 2$ (dotted line), $\rho_{12} = 10$ (dashed-dot line). (a) Weight-averaged molecular weight, (b) polydispersity index, and (c) fraction of dendritic units.

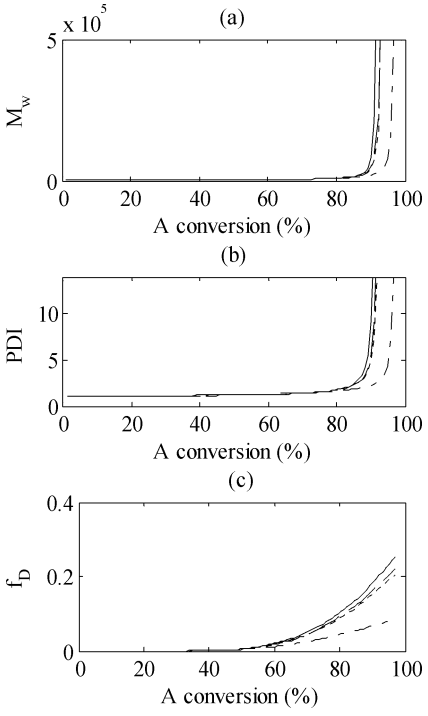

Figure 5. Simulated evolution with end-capping reagents added at the beginning of the process, with A_2:B_3:E = 1:1:1. The molecular weight of E (PPG-M-1000) is $M_{w,cap} = 1200$ g/mol. As in Figure 4, $\rho_{12} = k_1/k_2$ and $k_2 = k_3$. $r_{12} = 1$ (solid line), $\rho_{12} = 1.5$ (dashed line), $\rho_{12} = 2$ (dotted line), $\rho_{12} = 10$ (dashed-dot line). (a) Weight-averaged molecular weight, (b) polydispersity index, and (c) fraction of dendritic units. (Note: dendritic units are calculated here based on the number of A−B reactions. E−B reactions are not considered in the calculation since they do not lead to further branching.)

is measured by NMR. Curves are shown for the values of ρ_{12} considered previously in Figure 4. A primary observation is that the addition of the end-capping reagents has the larger effect

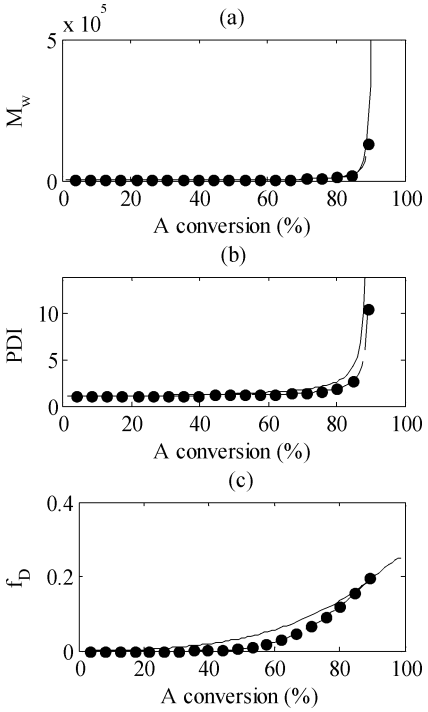

Figure 6. Simulated evolution with end-capping reagents added at the beginning of the process, with variation in stochiometry: A_2:B_3:E = 1:1:1 (solid line) and A_2:B_3:E = 1:0.9:1 (dotted line with markers). The molecular weight of E (PPG-M-1000) is $M_{w,cap} = 1200$ g/mol. $\rho_{12} = k_1/k_2 = 1.5$ and $k_2 = k_3$. (a) Weight-averaged molecular weight, (b) polydispersity index, and (c) fraction of dendritic units.

when the reactivity ratio is also large. Furthermore, this effect is only observed when the end-capping reagents also have a higher reactivity than the A groups in A_2 ($\epsilon \gg 1$). This might be the case for the dodecanol reagent if the end-capping reagent has a higher diffusivity than the A_2 due to its lower molar mass.

In the simulations presented in Figures 5 and 6, we set $\epsilon = 1000$, although the results are similar for $\epsilon = 10$. When $\epsilon \approx 1$, the simulations predict that the end-capping reagents have a negligible effect on the polymer structure. By reacting with the excess B groups, they only add their extra mass to the polymer. In the opposite limit, when $\epsilon \gg 1$ and $\rho_{12} \gg 1$, the E groups react quickly with the free B_3 monomers, after which the EB_3 units begin reacting with A_2. Each B_3 is thus bonded to only two A_2 monomers, so the polymers have a linear structure.

In the experiments, it was observed that the gel point was completely suppressed up to 98% conversion of each monomer, and the measured g' contraction factor from GPC was more consistent with a highly branched polymer (large f_D). Our simulations do predict a suppression of molecular weight with the end-capping reagents, but gelation is only delayed and not completely suppressed. At the extreme value $\rho_{12} = 10$, a significant reduction in f_D is also implied, but at lower values of ρ_{12}, high levels of branching are still predicted.

In the presentation of the experimental results,[1] we suggested that ester interchange of the A_2 with the monofunctional reagents might account for the observed reduction in molecular weight. While this interchange would cause a randomization of the polymer, at the high conversion of 98% it does not provide a consistent explanation for the extreme reduction in molecular weight. At 98% conversion, most of the A_2 monomers freed up by ester interchange would have reacted with another B_3 monomer.

Other effects not included in the model could be causing the suppression of gelation observed in the experiments, such as

the spatial distribution of the monomers in the polymer. These effects could be exacerbated when the end-capping reagents are added since all B groups must eventually react, even those buried or blocked in the center of the spherical polymer. Possibly, at high conversion, such groups are more likely to undergo cyclization reactions, which would suppress the molecular weight.

An alternative explanation was also suggested by our simulations. We observed that the simulation results are extremely sensitive to the stoichiometry near A_2:B_3:E = 1:1:1. In particular, if there is a reduction in the amount of B_3, then not all of the A_2 groups will be able to react with B groups, and the molecular weight will be reduced. This may be a particular issue in our experiments, since B_3 loss may be facilitated by the nitrogen purge at our final polymerization temperature of 180 °C. Because of the uncertainty in our final stoichiometry measurements, it is not possible to eliminate this effect. The simulations suggest that that our chosen stoichiometry of 1:1:1 is not a robust operating point due to the extreme sensitivity of the molecular weight on the stoichiometry. Figure 6 shows a comparison of the simulations with A_2:B_3:E = 1:1:1 and with 1:0.9:1. At this stoichiometry, 90% A_2 conversion is the maximum that can be achieved, and gelation is completely suppressed at full B_3 conversion.

V. Conclusions

The formation of highly branched poly(ether ester)s by the melt condensation of an A_2 oligomer with a B_3 monomer has been studied using experiments and kinetic Monte Carlo simulations. The simulations demonstrated that unequal reactivities can play an important role in the structure development of hyperbranched polymers, even when it has a little impact on the molecular weight. The results also indicate that the presence of end-capping reagents delays the gel point. However, the effect of end-capping agents also depends strongly on the ratios of the various monomers and their reactivity ratios. These results are motivating our further study of the role of end-capping reagents in the $A_2 + B_3$ system. In summary, the kinetic Monte Carlo simulations provide a tool for quantitatively assessing the effects of simple reaction mechanisms on molecular structure evolution, enabling the consideration of a broader range of mechanisms than with analytical models.

Acknowledgment. This material is based upon work supported by, or in part by, the U.S. Army Research Laboratory and the U.S. Army Research Office under contract/grant DAAD 19-02-1-0275, Macromolecular Architecture for Performance (MAP) MURI, and the Air Force Office of Scientific Research under award FA9550-04-1-1083. The authors also thank Eastman Chemical Co. for financial support and acknowledge Iskender Yilgor and Emel Yilgor for their role in initiating this collaboration.

References and Notes

(1) Unal, S.; Long, T. E. *Macromolecules* **2006**, *39*, 2788.
(2) Aerts, J. *Comput. Theor. Polym. Sci.* **1998**, *8*, 49.
(3) Kim, Y. H. *J. Polym. Sci., Part A: Polym. Chem.* **1998**, *36*, 1685.
(4) Voit, B. *J. Polym. Sci., Part A: Polym. Chem.* **2005**, *43*, 2679.
(5) Jikei, M.; Kakimoto, M. *Prog. Polym. Sci.* **2001**, *26*, 1233.
(6) Gao, C.; Yan, D. *Prog. Polym. Sci.* **2004**, *29*, 183.
(7) Jikei, M.; Chon, S. H.; Kakimoto, M. A.; Kavauchi, S.; Imase, T.; Watanabe, J. *Macromolecules* **1999**, *32*, 2061.
(8) Kricheldorf, H. R.; Vakhtangishvili, L.; Fritsch, D. J. *J. Polym. Sci., Part A: Polym. Chem.* **2002**, *40*, 2967.
(9) Fang, J.; Kita, H.; Okamoto, K. *Macromolecules* **2000**, *33*, 4639.
(10) Emrick, T.; Chang, H. T.; Frechet, J. M. J. *Macromolecules* **1999**, *32*, 6380.
(11) Komber, H.; Voit, B. I.; Monticelli, O.; Russo, S. *Macromolecules* **2001**, *34*, 5487.
(12) Lin, Q.; Long, T. E. *Macromolecules* **2003**, *36*, 9809.
(13) Yan, D.; Gao, C. *Macromolecules* **2000**, *33*, 7693.
(14) Kricheldorf, H. R.; Fritsch, D.; Vakhtangishvili, L.; Schwarz, G. *Macromolecules* **2003**, *36*, 5551.
(15) Unal, S.; Oguz, C.; Yilgor, E.; Gallivan, M.; Long, T. E.; Yilgor, I. *Polymer* **2005**, *46*, 4533.
(16) Flory, P. J. *Chem. Rev.* **1946**, *39*, 137.
(17) Dusek, K.; Duskova-Smrckova, M.; Voit, B. *Polymer* **2005**, *46*, 4265.
(18) Stockmayer, W. H. *J. Chem. Phys.* **1943**, *11*, 45.
(19) Stockmayer, W. H. *J. Polym. Sci.* **1952**, *9*, 69.
(20) Cail, J. I.; Stepto, R. F. T. *Polym. Bull. (Berlin)* **2007**, *58*, 15.
(21) Radke, W.; Litvinenko, G.; Muller, A. H. E. *Macromolecules* **1998**, *31*, 239.
(22) Holter, D.; Frey, H. *Acta Polym.* **1997**, *48*, 298.
(23) Hanselmann, R.; Holter, D.; Frey, H. *Macromolecules* **1998**, *31*, 3790.
(24) Zhou, Z. P.; Yan, D. Y. *Polymer* **2006**, *47*, 1473.
(25) Dusek, K.; Somvarky, J.; Smrckova, M.; Simonsick, W. J.; Wilczek, L. *Polym. Bull. (Berlin)* **1999**, *42*, 489.
(26) Deleted in proof.
(27) Gong, C.; Miravet, J.; Frechet, J. M. J. *J. Polym. Sci., Part A: Polym. Chem.* **1999**, *37*, 3193.
(28) Kricheldorf, H. R.; Schwarz, G. *Macromol. Rapid Commun.* **2003**, *24*, 359.
(29) Galina, H.; Lechowicz, J. B. *e-Polym.* **2002**, *12*, 1.
(30) Widmann, A. H.; Davies, G. R. *Comput. Theor. Polym. Sci.* **1998**, *8*, 191.
(31) Somvarsky, J.; Dusek, K. *Polym. Bull. (Berlin)* **1994**, *33*, 369.
(32) Cameron, C. *J. Chem. Phys.* **1998**, *108*, 8235.
(33) Stumbe, J.; Bruchmann, B. *Macromol. Rapid Commun.* **2004**, *25*, 921.
(34) Bortz, A. B.; Kalos, M. H.; Lebowitz, J. L. *J. Comput. Phys.* **1975**, *17*, 10.
(35) McKee, M. G.; Unal, S.; Wilkes, G. L.; Long, T. E. *Prog. Polym. Sci.* **2005**, *30*, 507.
(36) Somvarsky, J.; Dusek, K. *Polym. Bull. (Berlin)* **1994**, *33*, 377.
(37) Kricheldorf, H. R.; Lomadze, N.; Polefka, C.; Schwarz, G. *Macromolecules* **2006**, *39*, 2107.

MA070225V